A density functional theory study of the effects of metal cations on the Brønsted acidity of H-ZSM-5

Nick O. Gonzales, Arup K. Chakraborty [a] and Alexis T. Bell

Materials Sciences Division, Lawrence Berkeley Laboratory, and
Department of Chemical Engineering and Department of Chemistry [a], University of California, Berkeley, CA 94720, USA

Received 9 September 1997; accepted 10 December 1997

Density functional theory calculations have been carried out to establish the influence of mono- and polyvalent cations on the Brønsted acidity of H-ZSM-5. The zeolite was modeled as a cluster containing 41–45 atoms, in the center of which is an $Al^{(1)}(OH)SiOAl^{(2)}(OM)$ unit, where $M^+ = H^+, Li^+, Na^+, K^+, Ca(OH)^+, AlO^+, Al(OH)_2^+$. The local geometry of the Brønsted acid site is affected by the nature of M^+ and this in turn causes a change in the value of the proton affinity (PA) for the site. The highest value of PA is 330 kcal/mol for $M^+ = H^+$ and the lowest value of PA is 305 kcal/mol for $M^+ = AlO^+$. No correlation was found between the value of PA and the Mulliken charge on $Al^{(1)}$. With the exception of the case where $M^+ = AlO^+$, the binding energy of CO with the Brønsted acid proton is approximately 8.8 kcal/mol, independent of the nature of M^+. When $M^+ = AlO^+$, the binding energy for CO is 11.1 kcal/mol. The present calculations suggest that different factors affect proton affinity and the binding energy for CO adsorption.

Keywords: Brønsted acidity, zeolites, density functional theory

1. Introduction

Brønsted acid sites in zeolites occur in the form of bridging hydroxyl groups, viz., ≡Si(OH)Al≡. The acid strength of such sites is affected by a number of factors including the bond angle of the Si–O–Al triad, the presence or absence of Al atoms in T sites that are next-nearest neighbors to the Si atom in the Si–O–Al triad, and the presence of defects in the zeolite framework and extra-framework alumina located in proximity to the Brønsted acid site (see for example refs. [1–4]). It has also been proposed that polyvalent cations situated on charge exchange sites that are proximate to a Brønsted acid site can affect the strength of the latter site [5–7]. Of particular interest are the recent studies of Koningsberger and Miller [8] who report that the whiteline intensity at the K-edge of the Al X-ray absorption peak increases in the order H-Y < H-Ca-Y < H-LaY, paralleling the increasing strength of the Brønsted acidity. A similar correlation was observed for H-Y and steam dealuminated H-Y (H-USY), the latter material exhibiting the higher acidity [9]. The rise in the acidity of H-Y upon steaming was attributed to the occupation of cation exchange sites by extraframework alumina species, such as AlO^+. In both studies, it was hypothesized that the rise in acidity is attributable to the withdrawal of electron density from lattice oxygen caused by the increase in positive charge on the Al induced by the presence of a polyvalent cation on a charge-exchange site proximate to a Brønsted acid site.

While the interpretation offered by Koningsberger and Miller [8,9] is plausible, the experimental data alone cannot rule out the possibility that other factors also contribute to the rise in Brønsted acidity when metal cations are exchanged into the zeolite. This influence of changes in the local geometry and charge distribution near a Brønsted acid site can be examined, though, through quantum chemical calculations. Recent investigations have shown that calculations based on quantum density functional theory are particularly well suited for assessing such effects on the electronic properties of Brønsted acid sites in H-ZSM-5 and other zeolites [10–16]. Such calculations have also been used recently to demonstrate that defects in the form of silanol groups located on a Si atom bonded via a bridging oxygen atom to an Al atom can significantly lower the proton affinity (PA) of the associated Brønsted acid proton [4]. The present calculations were undertaken to determine whether monovalent and polyvalent cations located at charge-exchange sites proximate to a Brønsted acid site could affect the PA of the Brønsted acid proton. The effects of metal cations on the interactions of Brønsted acid protons with the weak base CO were also examined.

2. Theoretical approach

The Brønsted acid site in H-ZSM-5 is represented by a cluster containing 41 atoms with the acid center located near an Al atom in a T12 site [17]. The T12 site resides at the intersection of the straight channel and the sinusoidal channel, and has been identified in semiemperical calculations as the energetically preferred location for Al [18]. At the core of the cluster is an $\equiv Al^{(1)}(OH)SiOAl^{(2)}(OM)\equiv$ unit where $M^+ = H^+, Li^+, Na^+, K^+, Ca(OH)^+, AlO^+$, or $Al(OH)_2^+$. Hydrogen atoms are used to terminate the clusters. Each of the H atoms is located at a distance of 1 Å from the corresponding oxygen atom, and is oriented in the direction of the bond to the next silicon atom. With the exception of the terminating OH groups, all of the atoms in the cluster are allowed to relax geometrically during the course of the calculation. The initial positions of all atoms in the cluster are those determined for the high-temperature, orthorhombic form of H-ZSM-5 [17]. For the corresponding anion, the proton is removed from the optimized acid geometry and the anion geometry is then reoptimized.

Gradient corrected density functional theory (DFT) implemented within the PSGVB suite of programs [19] was used to determine cluster energies, geometries, and Mulliken populations. The B3LYP hybrid method [20] was used to represent the exchange and correlation energies. To minimize the computational time needed for a run, we first carried out Hartree–Fock (HF) geometry optimizations. These calculations provided the initial estimate of the cluster geometry for the more computationally demanding B3LYP calculations.

6-31G basis sets [21] were used for O, H, and Li while the effective core potentials (ECP) of Hay and Wadt [22], with the associated valence basis sets, were used for Si, Al, and the larger metal cations. No corrections were made for basis set superposition error, nor were zero point energy corrections accounted for in calculating energy differences.

The influence of local composition on Brønsted acidity was explored in two ways. The first involved calculation of the proton affinity (PA), which is the difference in energy between the protonated and deprotonated forms of the cluster. The second was based on a calculation of the heat of adsorption of CO, a weak base. While both methods provide a means for identifying the effects of local composition on zeolite acidity, the trends in acidity with composition may not be the same. The reason for this is that while PA is influenced significantly by the relaxation energy of the anion, this effect does not contribute to the heat of CO adsorption.

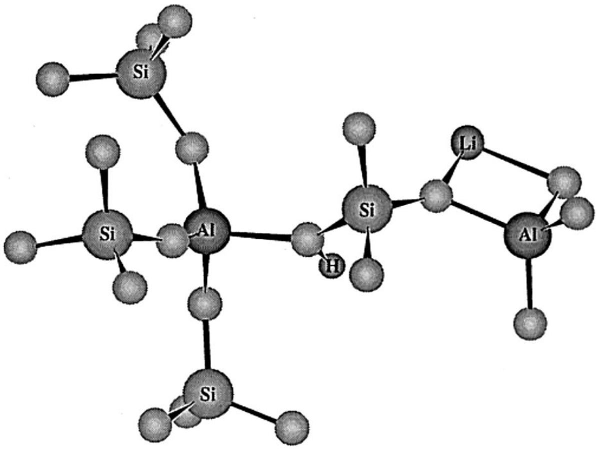

Figure 2. Structure of the cluster containing $M^+ = Li^+$. PA = 324. The terminal hydrogen atoms are not shown for the sake of clarity.

3. Results and discussion

Figures 1–7 show the equilibrium structures of the seven protonated clusters investigated. Selected bond distances and angles for these structures are presented in table 1, together with the Mulliken charges associated with H, O, and $Al^{(1)}$. Substitution of the proton associated with $Al^{(2)}$ by either a monovalent or polyvalent cation causes a number of small changes in the geometry of the $\equiv Al^{(1)}(OH)Si\equiv$ unit associated with the Brønsted acid site. The most significant of these changes is in the magnitude of $\gamma_{dihedral}$, the angle between the OH bond

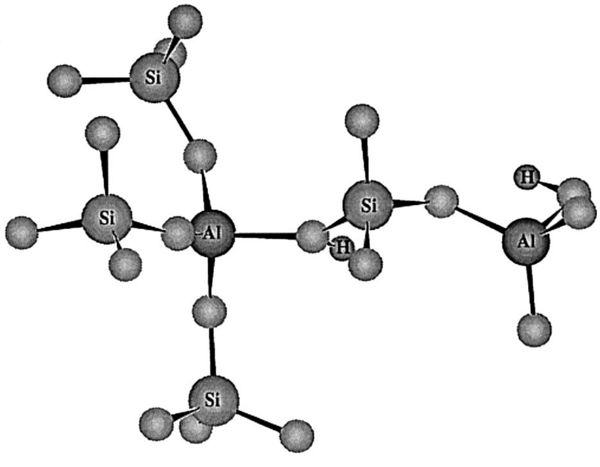

Figure 1. Structure of the cluster containing $M^+ = H^+$. PA = 330. The terminal hydrogen atoms are not shown for the sake of clarity.

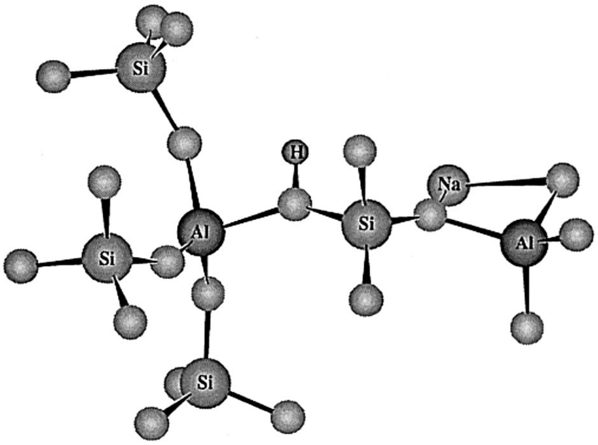

Figure 3. Structure of the cluster containing $M^+ = Na^+$. PA = 309. The terminal hydrogen atoms are not shown for the sake of clarity.

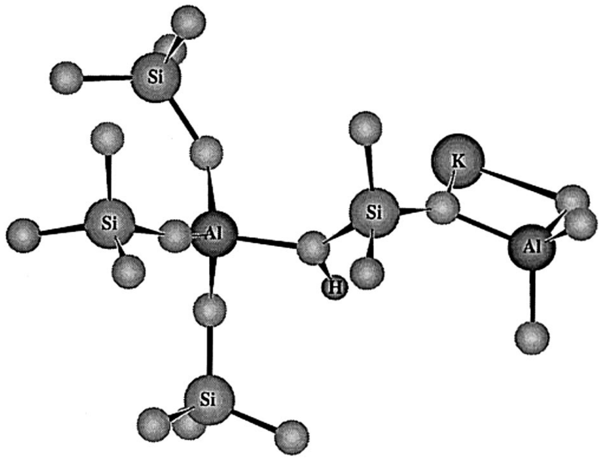

Figure 4. Structure of the cluster containing $M^+ = K^+$. PA = 314. The terminal hydrogen atoms are not shown for the sake of clarity.

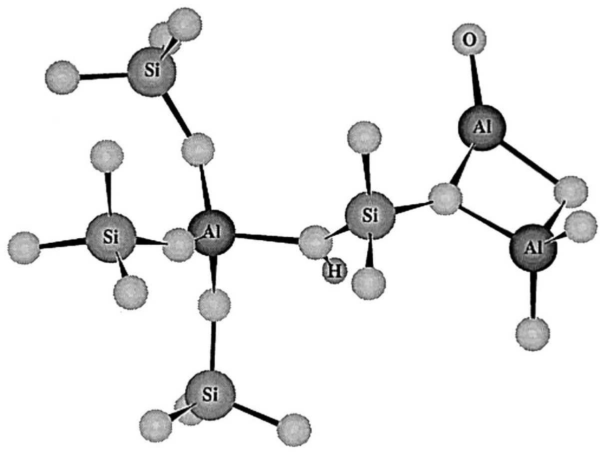

Figure 6. Structure of the cluster containing $M^+ = AlO^+$. PA = 305. The terminal hydrogen atoms are not shown for the sake of clarity.

and the Al–O–Si plane. It is evident that cation substitution for H^+ causes a series of subtle structural changes in the cluster which ultimately results in reorientation of the OH bond relative to the Al–O–Si plane. Table 1 also shows that cation substitution has relatively little effect on the Mulliken charges for H and O, with the exception of the case where the cation is $Al(OH)_2^+$. The perturbation observed in the latter case may be due to hydrogen bonding between the Brønsted acid proton and one of the OH groups on the $Al(OH)_2^+$ cation. Changes in the Mulliken charge on Al$^{(1)}$ are observed, but these are relatively small.

In calculating the equilibrium structure of the anionic form of the cluster, it was observed that for H^+, Li^+, AlO^+, and $Al(OH)_2^+$, the position of the cation in the anion was essentially the same as that in the protonated structures. However, for Na^+, K^+, and $Ca(OH)^+$, the cation was observed to move so as to straddle the two O atoms bonded to the Si atom in the $\equiv$Al–O$^-$–Si–O$^-$–Al$\equiv$ portion of the cluster. For these larger cations, the distance between the cation and Al$^{(2)}$ is sufficiently large that the cation–framework interaction energy is smaller when the cation moves so as to interact with the O atoms attached to the Si atom located between the two Al atoms.

The influence of substituting the proton associated with Al$^{(2)}$ by a mono- or polyvalent cation on the PA of the proton associated with Al$^{(1)}$ is given in table 1. It is evident that the value of PA is highest when $M^+ = H^+$ and that PA decreases in the order $H^+ > Li^+ > Al(OH)_2^+ > K^+ > Na^+ > AlO^+ > Ca(OH)^+$, corresponding to an increase in Brønsted acidity. The decrease in PA is paralleled by a decrease in the HOMO–LUMO gap (see table 2), indicating an increasing softness of the acid [23]. The rise in Brønsted acidity (i.e., lowering of the value of PA) for H-ZSM-5 upon the introduction of $Ca(OH)^+$ or

Figure 5. Structure of the cluster containing $M^+ = Ca(OH)^+$. PA = 303. The terminal hydrogen atoms are not shown for the sake of clarity.

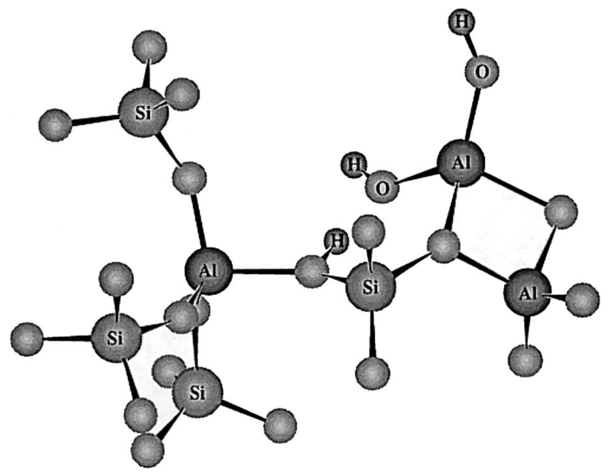

Figure 7. Structure of the cluster containing $M^+ = Al(OH)_2^+$. PA = 322. The terminal hydrogen atoms are not shown for the sake of clarity.

Table 1
Geometries, Mulliken charges. and proton affinity for clusters of the form $Al^{(1)}(OH)SiOAl^{(2)}(OM)$ [a]

M^+	R_{OH}	$R_{Al^{(1)}H}$	$R_{Al^{(1)}O}$	R_{SiO}	$\alpha_{Al^{(1)}OSi}$	$\alpha_{Al^{(1)}OH}$	$\gamma_{dihedral}$	Al	O	H	PA
H^+	0.975	2.360	1.807	1.692	134.6	112.6	16.0	1.71	−0.99	0.49	330
Li^+	0.974	2.339	1.814	1.699	134.1	110.4	3.0	1.74	−1.00	0.48	324
Na^+	0.979	2.196	1.793	1.695	142.3	100.6	22.5	1.74	−0.99	0.47	309
K^+	0.975	2.328	1.806	1.715	134.8	110.9	−5.8	1.75	−1.00	0.47	314
$Ca(OH)^+$	0.977	2.328	1.824	1.701	133.4	108.6	−8.8	1.74	−1.00	0.49	303
AlO^+	0.977	2.316	1.848	1.678	131.5	106.0	−3.9	1.73	−0.99	0.49	305
$Al(OH)_2^+$	1.062	2.434	1.816	1.668	129.1	112.9	22.8	1.70	−1.07	0.57	322

[a] All bond distances are given in Å and all bond angles in degrees. Mulliken charges are given in units of $|e|$. Proton affinities are given in units of kcal/mol.

AlO^+ is qualitatively similar to what has been reported by Koningsberger and Miller for H-Y zeolite [9]. However, in contrast to the findings of these authors, we observe that while the Mulliken charge on $Al^{(1)}$ increases upon replacement of the proton associated with $Al^{(2)}$ by a metal cation, there appears to be no correlation between the charge on $Al^{(1)}$ and PA for any of the cases studied.

The effect of cation substitution on the binding energy of CO is listed in table 2. If the charge compensating cation for $Al^{(2)}$ is H^+, the CO binding energy is 8.8 kcal/mol. This value is about 2.4 kcal/mol higher than that reported by Farnworth and O'Malley [24] based on DFT calculations carried out with an $H_3Al(OH)SiH_3$ cluster using the B3LYP functional to represent the effects of exchange and correlation, and the 6-31G** basis set. After correction for the zero-point energy and basis-set-superposition error, these authors estimate the corrected adsorption energy to be 2.62 kcal/mol, which is slightly lower than the experimental range of 3.25–4.10 kcal/mol for H-X zeolite [25]. In the present study, no corrections were made for basis-set-superposition error, since they are expected to be roughly the same for each of the clusters examined, and we are only interested in the trends in CO binding energy with the nature of the substituted cation.

While the substitution of H^+ by Li^+ has no effect on the binding energy of CO, the introduction of AlO^+ increases the binding energy to 11.1 kcal/mol. This increase parallels the decreases in PA_e and the decrease in the energy of the HOMO–LUMO gap when AlO^+ is substituted for H^+. Table 2 also shows that, consistent with the higher binding energy of CO when AlO^+ is the charge compensation cation, the H–C bond distance is shorter and the C–O bond distance is longer. It is also observed that when K^+ or $Ca(OH)^+$ is the charge-compensating cation, the binding energy for CO is essentially the same as that calculated when H^+ is the charge compensating cation. Thus, in these two instances, there seems to be no correlation between the CO binding energy and the PA. Since the influence of anion relaxation is especially large for these cases, due to the shift in the positions of K^+ and $Ca(OH)^+$ relative to the zeolite framework upon going from the protonated to the deprotonated (anionic) form of the zeolite, the decrease in the value of PA relative to the situation in which the second charge compensating cation is H^+ may be exaggerated. For this reason, the heat of adsorption of CO may provide a more appropriate measure of the effects of metal cations on the Brønsted acidity of ZSM-5 than does PA in such instances.

4. Conclusions

The substitution of mono- or polyvalent cations for H^+ as the charge compensating cation for an Al atom located in next-nearest neighbor proximity to a Brønsted acid site in H-ZSM-5 causes a number of changes to the local geometry of the Brønsted acid site, as well as a

Table 2
Geometries, binding energies, and HOMO–LUMO gaps for CO interactions with Brønsted acid sites in clusters of the form $Al^{(1)}(OH)SiOAl^{(2)}(OM)$ [a]

M^+	R_{HC}	α_{HCO}	ΔR_{CO}	ΔE_{CO}	$\Delta E_{HOMO-LUMO}$	PA
H^+	1.980	172.2	0.003	8.7	139	330
Li^+	1.998	174.9	0.003	8.7	123	324
Na^+	na	na	na	na	115	309
K^+	2.084	171.5	0.002	8.0	115	314
$Ca(OH)^+$	2.025	163.5	0.005	8.5	115	303
AlO^+	1.890	167.7	0.006	11.1	105	305
$Al(OH)_2^+$	na	na	na	na	131	322

[a] All bond distances are given in Å and all bond angles in degrees. CO binding energies, HOMO–LUMO gaps, and proton affinities are given in units of kcal/mol.

change in the positive charge density of the Al atom associated with the site. These changes result in a reduction in the PA of the Brønsted-acid proton, suggesting an increase in its acid strength. For the systems investigated, these changes are most notable when the substituting cation is AlO^+. Substitution of AlO^+ for H^+ also causes an increase in the binding energy for CO. However, it is observed that in general there seems to be no clear correlation between the PA and the binding energy of CO. This may be due at least in part to the influence of anion relaxation effects, which can be large particularly when the charge compensating metal cation shifts position as the zeolite goes from its protonated to its deprotonated state. It is concluded therefore that different aspects of the local structure and composition of H-ZSM-5 affect the proton affinity and the binding energy of the proton with weak bases.

Acknowledgement

This work was supported by a grant from the Office of Industrial Technology of the US Department of Energy under Contract DE-AC03-76SF00098. Computing resources were provided by the National Energy Research Supercomputing Center and the San Diego Supercomputing Center.

References

[1] V.B. Kazansky, Catal. Today 3 (1988) 367.

[2] E.F. Rakiewicz, K.T. Mueller, T.P. Javie, K.J. Sutovich, T.G. Roberie and A.W. Peters, Microporous Mater. 7 (1996) 81.

[3] E. Brunner, H. Ernst, D. Freude, T. Frohlich, M. Hunger and H. Pfeifer, J. Catal. 127 (1991) 34.

[4] N.O. Gonzales, A.K. Chakraborty and A.T. Bell, J. Phys. Chem., in press.

[5] P.O. Fritz and J.H. Lunsford, J. Catal. 119 (1989) 85.

[6] R. Carvajal, P.-J. Chu and J.H. Lunsford, J. Catal. 125 (1990) 123.

[7] J.H. Lunsford, *Fluid Catalytic Cracking II, Concepts in Catalyst Design*, ACS Symp. Ser. 452 (1991) 1.

[8] D.C. Koningsberger and J.T. Miller, in: *Zeolites: A Refined Tool for Designing Catalytic Sites*, eds. L. Bonneviot and S. Kaliaguine (Elsevier, Amsterdam, 1995) p. 125.

[9] D.C. Koningsberger and J.T. Miller, in: *Studies in Surface Science and Catalysis*, Vol. 101, eds. J.W. Hightower, W.N. Delgass, E. Iglesia and A.T. Bell (Elsevier, Amsterdam, 1996) p. 841.

[10] H.V. Brand, L.A. Curtiss and L.E. Iton, J. Phys. Chem. 96 (1992) 7725.

[11] H.V. Brand, L.A. Curtiss and L.E. Iton, J. Phys. Chem. 97 (1992) 12773.

[12] A.E. Alvarado-Swaisgood, M.K. Barr, P.J. Hay and A. Redondo, J. Phys. Chem. 95 (1991) 10031.

[13] J.B. Nicholas, in: *Studies in Surface Science and Catalysis*, Vol. 101, eds. J.W. Hightower, W.N. Delgass, E. Iglesia and A.T. Bell (Elsevier, Amsterdam, 1996) p. 1263.

[14] J.B. Nicholas, R.E. Winans, R.J. Harrison, L.E. Iton, L.A. Curtiss and A.J. Hopfinger, J. Phys. Chem. 96 (1992) 10247.

[15] G.J. Kramer and R.A. van Santen, J. Am. Chem. Soc. 115 (1993) 2887.

[16] A. Kyrlidis, S.J. Cook, A.K. Chakraborty, A.T. Bell and D.N. Theodorou, J. Phys. Chem. 99 (1995) 1505.

[17] D.H. Olson, G.T. Kokotailo, S.L. Lawton and W.M. Meirer, J. Phys. Chem. 85 (1981) 2238.

[18] S. Lonsinger, A.K. Chakraborty, D.N. Theodorou and A.T. Bell, Catal. Lett. 11 (1991) 209.

[19] M.N. Ringnalda, J.-M. Langlois, R.B. Murphy, B.H. Greeley, C. Cortis, T.V. Russo, B. Marten, R.E. Donnelly Jr., W.T. Pollard, Y. Cao, R.P. Muller, D.T. Mainz, J.R. Wright, G.H. Miller, W.A. Goddard III and R.A. Friesner, PS-GVB v2.3, Schrodinger, Inc. (1996).

[20] (a) A.D. Becke, J. Chem. Phys. 98 (1993) 5648;
(b) C. Lee, W. Yang and R.G. Parr, Phys. Rev. B 37 (1988) 785.

[21] (a) W.J. Hehre, R. Ditchfield and J.A. Pople, J. Chem. Phys. 56 (1972) 2257;
(b) J.D. Dill and J.A. Pople, J. Chem. Phys. 62 (1975) 2921;
(c) J.S. Binkley and J.A. Pople, J. Chem. Phys. 66 (1977) 879.

[22] (a) P.J. Hay and W.R. Wadt, J. Chem. Phys. 82 (1985) 270;
(b) P.J. Hay and W.R. Wadt, J. Chem. Phys. 82 (1985) 284.

[23] R.G. Pearson, J. Am. Chem. Soc. 85 (1963) 3533.

[24] K.J. Farnworth and P.J. O'Malley, J. Phys. Chem. 100 (1996) 1814.

[25] N.M. Gupta, V.S. Kamble, K.A. Rao and R.M. Iyer, J. Catal. 120 (1989) 432.